

Estimating intermittency exponent in neutrally stratified atmospheric surface layer flows: A robust framework based on magnitude cumulant and surrogate analyses

Sukanta Basu^{a)}

Department of Geosciences, Texas Tech University, Lubbock, Texas 79409, USA

Efi Foufoula-Georgiou^{b)} and Bruno Lashermes

St. Anthony Falls Laboratory, University of Minnesota, Minneapolis, Minnesota 55414, USA

Alain Arnéodo

Laboratoire de Physique, Ecole Normale Supérieure de Lyon - CNRS, 46 Allée d'Italie, 69364 Lyon cédex 07, France

(Received 18 January 2007; accepted 23 August 2007; published online 7 November 2007)

This study proposes a novel framework based on magnitude cumulant and surrogate analyses to reliably detect the presence of intermittency and estimate the intermittency coefficient from short-length coarse-resolution turbulent time series. Intermittency coefficients estimated from a large number of neutrally stratified atmospheric surface layer turbulent series from various field campaigns are shown to remarkably concur with well-known laboratory experimental results. In addition, surrogate-based hypothesis testing significantly reduces the likelihood of detecting a spurious nonzero intermittency coefficient from nonintermittent series. The discriminatory power of the proposed framework is promising for addressing the unresolved question of how atmospheric stability affects the intermittency properties of boundary layer turbulence. © 2007 American Institute of Physics. [DOI: 10.1063/1.2786001]

I. INTRODUCTION

Existence of small-scale intermittency is an intriguing yet unsettled topic in contemporary turbulence research. Over a number of decades, researchers have been trying to unravel intermittency in turbulence measurements and at the same time formulating diverse conceptual models to rationalize the observed intermittency.^{1,2} Encouragingly, “practical” implications of intermittency research outcomes are also being appreciated by the numerical turbulence modeling community and a critical knowledge transfer is taking place, as evidenced by the recent literature.^{3–7}

One of the most widely used statistics characterizing the intermittent nature of turbulence is the so-called “intermittency exponent” (μ).⁸ From observational data, μ can be estimated directly or indirectly via several methods. The direct estimates typically involve appropriate characterization of the second-order scaling behavior of the local rate of energy dissipation (ε) field. In this respect, several alternatives (e.g., second-order integral moment, two-point correlation function, spectral density) are available in the literature.^{9–11} Recently, Cleve *et al.*¹² showed that among various direct approaches, the two-point correlation function $\langle \varepsilon(x+r)\varepsilon(x) \rangle$ of the energy dissipation field provides the most reliable estimates of μ . In this case, one can write

$$\langle \varepsilon(x+r)\varepsilon(x) \rangle \sim r^{-\mu}, \quad (1)$$

where r is within the inertial range. Here, the angular brackets denote spatial averaging.

The direct intermittency exponent estimation methods (based on ε) require very high-resolution (resolving on the order of Kolmogorov scale) data series of pristine quality. Most commonly, fast-response hot-wire measurements are used for this purpose.^{10–14} However, acquisition of hot-wire data in a natural setting could be quite challenging. For example, in the case of atmospheric boundary layer (ABL) field experiments, one needs to perform meticulous hot-wire calibration at short regular intervals in order to account for the ever changing (diurnally varying) ABL flow parameters.^{15,16}

The ABL community widely uses sonic anemometers for turbulent flux measurements in fields. In contrast to hot wires, these sensors require much lesser periodic calibration and maintenance. Unfortunately, path lengths (~ 10 cm) and sampling rate (~ 20 Hz) of conventional sonic anemometers are too coarse for direct μ estimation. In this paper, we will explore if sonic anemometer measurements, in lieu of hot-wire data, can be reliably used for indirect estimation of μ .

One of the most popular indirect μ estimation methods is associated with the scaling of sixth-order structure function.^{13,14,17} With certain plausible assumptions, one can show that¹⁷

^{a)}Also at the Wind Science and Engineering Research Center. Electronic mail: sukanta.basu@ttu.edu

^{b)}Also at the National Center for Earth Surface Dynamics.

$$S_6(r) = \langle [u(x+r) - u(x)]^6 \rangle = \langle (\Delta u)^6 \rangle \sim r^{2-\mu} \langle \varepsilon(x) \varepsilon(x+r) \rangle. \quad (2)$$

Using Eqs. (1) and (2), one gets $\langle (\Delta u)^6 \rangle \sim r^{2-\mu}$. Chambers and Antonia¹⁴ used this relatively simple indirect approach and obtained $\mu \sim 0.2$ in the atmospheric surface layer. From an adequate statistical convergence standpoint, estimation of higher-order (specifically, sixth-order in this context) structure functions require a very long time series.¹³ For instance, Chambers and Antonia¹⁴ used several runs of 15 min duration at a hot-wire sampling frequency of ~ 1.2 kHz (i.e., $\sim 10^6$ samples per series). On the other hand, 15–30 min sonic anemometer-based ABL turbulence series would typically consist of only 20 000 to 40 000 samples. Understandably, the estimates of μ from sonic anemometer series using the traditional sixth-order structure function approach will not be very reliable. This motivates us to use an alternative estimation approach, called the magnitude cumulant analysis, recently introduced by Delour *et al.*¹⁸ Using this approach and under the assumption of log-normality (as supported by our observational data), only second-order magnitude cumulants (rather than data-intensive sixth-order structure functions) are needed to estimate the intermittency coefficient (μ).

The interrelated objectives of this paper are twofold:

- (1) Assess the potential of the magnitude cumulant analysis in detecting and estimating intermittency from short-length coarse-resolution (sonic anemometer-acquired) ABL measurements.
- (2) Design a rigorous hypothesis-testing framework that would reduce the likelihood of spurious detection of a nonzero μ from nonintermittent (monofractal) series.

The paper is structured as follows. In Sec. II, we briefly describe the magnitude cumulant analysis technique. The iterative amplitude adjusted Fourier transform (IAAFT) algorithm-based surrogate analysis, originally developed by the chaos theory community for detection of nonlinearity in time series,¹⁹ is shown to be very robust and reliable for intermittency hypothesis testing. The IAAFT algorithm is presented in Sec. III. An extensive collection of observational data from various field campaigns is used in this study; Sec. IV provides brief description of these field datasets. Comprehensive results of intermittency estimation are presented in Sec. V and compared with published literature wherever possible. Lastly, Sec. VI summarizes our results and discusses perspectives for future research on the intriguing question of how atmospheric stability affects intermittency properties of boundary layer turbulence.

II. MAGNITUDE CUMULANT ANALYSIS

In the turbulence literature, the scaling exponent spectrum ζ_q is defined as

$$S_q(r) = \langle |\Delta u|^q \rangle \sim r^{\zeta_q}, \quad (3)$$

where $S_q(r)$ is the so-called q th-order structure function. As before, the angular bracket denotes spatial averaging and r is a separation distance that varies within the inertial range. If

the scaling exponent ζ_q is a nonlinear function of q , then the field is called “multifractal”; otherwise it is termed “monofractal.”^{1,20} In the traditional structure function approach, estimation of μ ($=2-\zeta_6$) requires a log-log plot of $S_6(r)$ versus r and subsequent extraction of the slope using a least-squares linear regression fit over a scaling regime (the inertial range). For a short time series, computation of $S_6(r)$ is problematic due to statistical convergence. An alternative reliable method, first advocated by Delour *et al.*,¹⁸ is to use the magnitude cumulant analysis. In this approach, the relationship between the moments of velocity increments (Δu) and the magnitude cumulants (C_n) reads as^{18,21}

$$\langle |\Delta u|^q \rangle = \exp\left(\sum_{n=1}^{\infty} C_n(r) \frac{q^n}{n!}\right), \quad (4)$$

where

$$C_1(r) \equiv \langle \ln|\Delta u| \rangle \sim -c_1 \ln(r), \quad (5a)$$

$$C_2(r) \equiv \langle (\ln|\Delta u|)^2 \rangle - \langle \ln|\Delta u| \rangle^2 \sim -c_2 \ln(r), \quad (5b)$$

$$C_3(r) \equiv \langle (\ln|\Delta u|)^3 \rangle - 3\langle (\ln|\Delta u|)^2 \rangle \langle \ln|\Delta u| \rangle + 2\langle \ln|\Delta u| \rangle^3 \sim -c_3 \ln(r). \quad (5c)$$

From Eqs. (3)–(5), it is straightforward to express the scaling exponent spectrum as¹⁸

$$\zeta_q = -\sum_{n=1}^{\infty} c_n \frac{q^n}{n!}. \quad (6)$$

We would like to point out that the magnitude cumulant analysis implicitly assumes that the ζ_q spectrum does not display any nonanalyticity.

Furthermore, by invoking a relationship between velocity increments (Δu) and local rate of dissipation fields (ε) [similar to Eq. (2)], for log-normal processes, one can arrive at²²

$$\mu \approx 9c_2. \quad (7)$$

Therefore, estimation of the intermittency exponent μ (for log-normal processes) would only require the computation of second-order magnitude cumulant; i.e., the second central moment of $\ln|\Delta u|$ [Eq. (5b)].

For large separation ($r \rightarrow L_i$, where L_i is the integral length scale), it is well documented that the probability distribution function (pdf) of velocity increments (Δu) approaches a Gaussian distribution. For this scenario, the following results can be derived analytically:

$$C_1(r) \rightarrow \frac{1}{2}[-\gamma - \ln(2)] = -0.64, \quad (8a)$$

$$C_2(r) \rightarrow \pi^2/8 = 1.23, \quad (8b)$$

$$C_3(r) \rightarrow -\frac{7}{4}\zeta(3) = -2.1, \quad (8c)$$

where γ is the Euler Gamma constant=0.577 216, and $\zeta(3)$ is Apéry’s constant=1.202 056 9. These asymptotic values of $C_1(r)$, $C_2(r)$, and $C_3(r)$ would be very useful to demarcate scaling regions in the case of short-length time series.

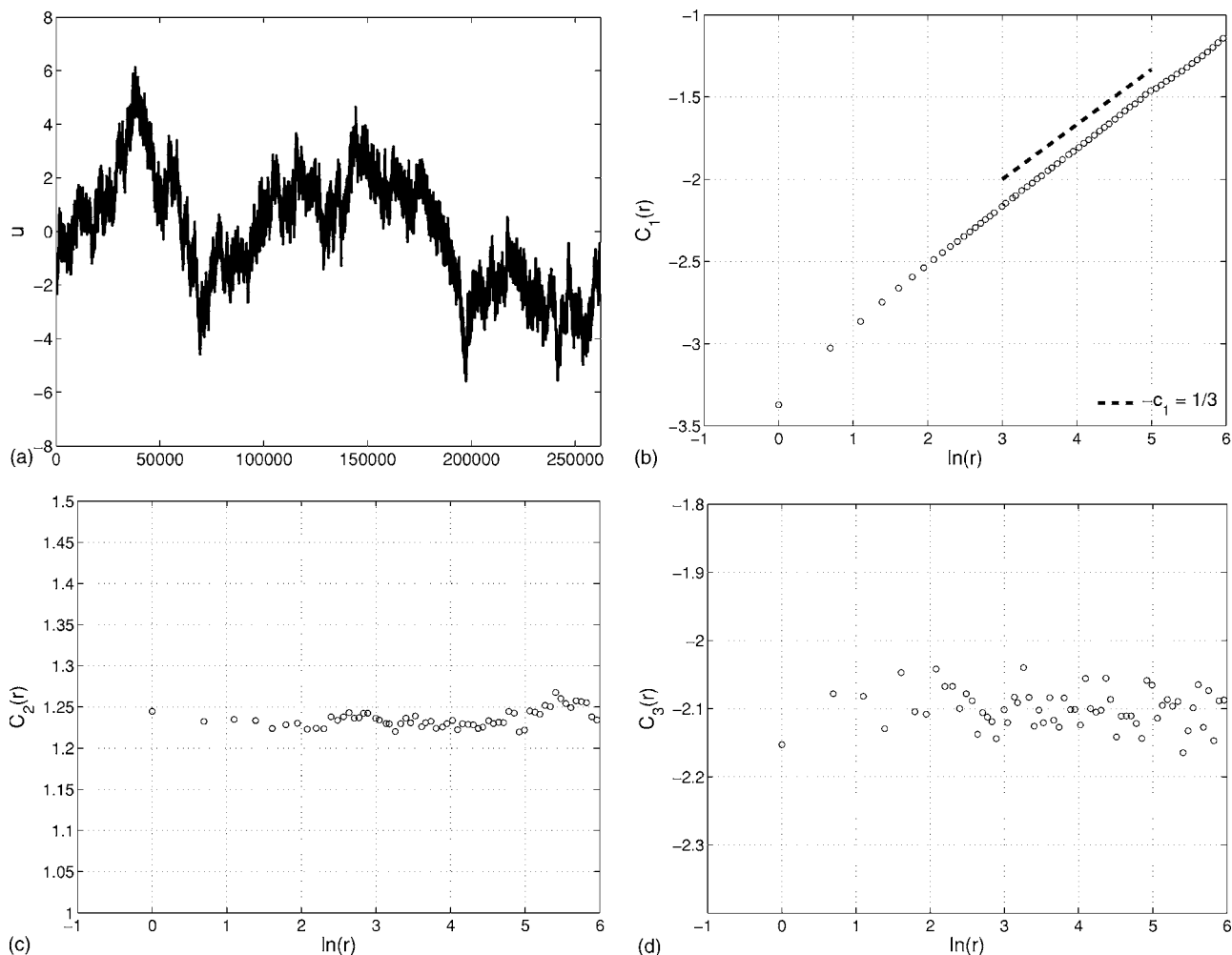


FIG. 1. A synthetic fractional Brownian motion ($h=1/3$) (top-left). The magnitude cumulants $C_1(r)$ (top-right), $C_2(r)$ (bottom-left), and $C_3(r)$ (bottom-right) are also shown. The dashed line in the top-right subplot shows the slope $-c_1=1/3$.

It is noted that instead of a physical space-based magnitude cumulant analysis approach [i.e., Eqs. (4) and (5)], one could also use wavelet-based magnitude cumulant analysis (see Venugopal *et al.*^{23,24} for a geophysical application). A wavelet-based approach becomes necessary for nonstationary signals and signals with Hölder exponents (h) outside the window of $[0, 1]$.^{25,26} In turbulence, $\langle h \rangle$ is close to K41 value of $1/3$, and to best of our knowledge is always found to be within the window of $h \in [0, 1]$.^{27,28} In addition, the ζ_q spectrum has never been reported to be nonanalytical in nature. Thus, in the present study we decided to employ physical space-based magnitude cumulant analysis approach.

Magnitude cumulant analysis of a synthetic fractional Brownian motion with $h=1/3$ (which displays K41 like $k^{-5/3}$ spectrum) is shown in Fig. 1. The dashed line in $C_1(r)$ versus $\ln(r)$ plot has the expected slope of $1/3$. For almost the entire scaling range, both $C_2(r)$ and $C_3(r)$ remain close to the theoretical Gaussian values of 1.23 and -2.1 , respectively. This signal does not show any sign of multifractality (expected) as the slope of $C_2(r)$ versus $\ln(r)$ cannot be claimed to be different from zero.

III. SURROGATE ANALYSIS

Noise is omnipresent in any measured signal, and turbulence signals are no exceptions. In addition to noise, limited amount of data (finite sample settings) in most field measurements could challenge intermittency detection and estimation even with the magnitude cumulant analysis method (e.g., assessment of a small nonzero slope in the $C_2(r)$ versus $\ln(r)$ plots). In this paper, we utilize a hypothesis-testing framework, based on surrogate analysis, in conjunction with magnitude cumulant analysis, for detecting and accurately estimating intermittency from short-length sonic anemometer measurements.

The concept of surrogates (stochastic realizations that preserve only certain characteristics of a process) was introduced into the chaos theory literature to provide a rigorous statistical test for the null hypothesis that an observed time series has been generated by a linear stochastic process (see Theiler *et al.*,²⁹ Kantz and Schreiber,³⁰ Basu and Foufoula-Georgiou,³¹ and the references therein). Over the years, several varieties of surrogates (randomly shuffled surrogates, Fourier phase randomized surrogates, iterative am-

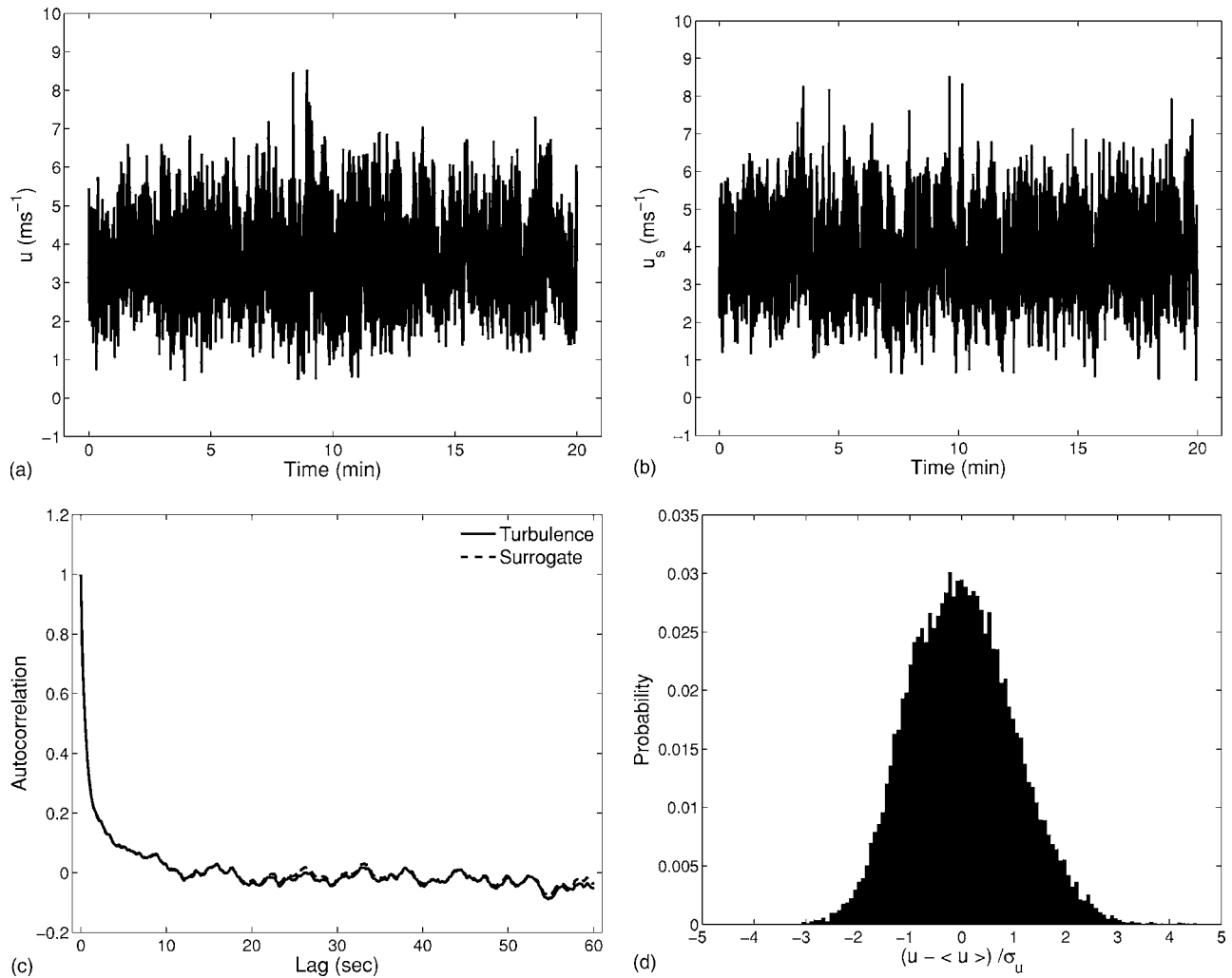


FIG. 2. Longitudinal velocity time series measured by a sonic anemometer (top-left) and its surrogate series generated by IAAFT methodology (top-right). Both series have approximately the same autocorrelation (bottom-left) and exactly the same probability density function (bottom-right).

plitude adjusted Fourier transform surrogates, stochastic IAAFT surrogates, and so on) have been proposed in the literature.³² In this paper, we will use the IAAFT algorithm proposed by Schreiber and Schmitz.¹⁹ IAAFT surrogates preserve the correlation structure (and, thus, the power spectrum due to the Wiener-Khinchin theorem) and the probability density function of a given time series. Apart from nonlinearity detection,^{19,31} the IAAFT surrogates have also been used to define a precipitation forecast quality index,³³ and to generate synthetic cloud fields.³⁴

In the turbulence literature, surrogate analysis-based hypothesis testing is virtually nonexistent with an exception of the paper by Nikora *et al.*³⁵ They used simple Fourier phase randomization approach (pdf of the original turbulence series was not preserved) in identifying the effects of turbulence intermittency and spectral energy flux. In comparison to the Fourier phase randomized approach, the IAAFT algorithm used in the present study designs stronger statistical test (due to its ability to preserve the integral pdf of the original signal) for the null hypothesis that an observed turbulence series is nonintermittent.

In Fig. 2, a sonic anemometer turbulence series and its

IAAFT surrogate are shown. By construction, they have the same pdf (bottom-right plot of Fig. 2) and virtually indistinguishable autocorrelation function (bottom-left plot of Fig. 2). Basic properties of the original turbulence series and its surrogate are provided in Table I. T_i and L_i denote integral time and length scales, respectively.

$$T_i = \int_0^{\infty} R(\tau) d\tau, \quad (9a)$$

$$L_i = U \cdot T_i, \quad (9b)$$

where $R(\tau)$ is the autocorrelation function. From Fig. 2 and Table I, we can safely infer that the IAAFT surrogate cap-

TABLE I. Basic statistics of a sonic anemometer turbulence series and its surrogate.

Series type	U (ms ⁻¹)	σ_u (ms ⁻¹)	T_i (s)	L_i (m)
Turbulence	3.73	1.06	1.47	5.47
Surrogate	3.73	1.06	1.46	5.43

TABLE II. Mean flow characteristics of the field measurements.

Sensor Type	z (m)	U (ms ⁻¹)	σ_u (ms ⁻¹)	T_i (s)	L_i (m)
Hot-wire anemometer	2.01	5.99	0.74	5.71	34.22
Sonic anemometer	0.96–4.28	1.60–7.30	0.34–1.57	1.08–9.09	2.57–33.22

tures the integral pdf and autocorrelation function of the original velocity series rather accurately. Later on, we will show that the IAAFT surrogates do not have the ability to capture the scale-dependent pdfs of velocity increments and this forms the basis for the proposed intermittency hypothesis testing.

IV. DESCRIPTION OF DATA

In this study, we primarily made use of an extensive atmospheric boundary layer turbulence dataset (comprising of sonic anemometer measurements) collected by various researchers from Johns Hopkins University, and the University of California-Davis during Davis 1994, 1995, 1996, and 1999 field studies. Comprehensive description of these field experiments (e.g., surface cover, fetch, instrumentation, sampling frequency) can be found in Pahlow *et al.*³⁶ Briefly, the collective attributes of the field dataset explored in this study are as follows: (i) surface cover: bare soil, and beans; (ii) sampling frequency: 18 to 21 Hz; (iii) sampling period: 20 to 30 min; (iv) sensor height (z): 0.96 to 4.28 m.

The ABL field measurements are seldom free from mesoscale disturbances, wave activities, nonstationarities, etc. The situation could be further aggravated by several kinds of sensor errors (e.g., random spikes, amplitude resolution error, drop outs, discontinuities, etc.). Thus, stringent quality control and preprocessing of field data are of utmost importance for any rigorous statistical analysis. Our quality control and preprocessing strategies are described in detail in Basu *et al.*³⁷ After the quality control and preprocessing steps, we were left with 139 “reliable” near-neutral ($|z/L| \leq 0.05$, where z is the sensor height and L denotes the Monin-Obukhov length) sets of runs for estimating the intermittency exponents.

We also estimated μ from a fast-response (10 kHz) hot-wire ABL turbulence series utilizing the magnitude cumulant analysis. The hot-wire measurements were taken at the Surface Layer Turbulence and Environmental Science Test (SLTEST) facility located in the western Utah Great Salt Lake desert under near-neutral atmospheric condition.^{15,16} In the following section, we will show that the intermittency exponent and other relevant statistics derived from this high Reynolds number (Re) hot-wire measurement are surprisingly similar to various published lower Re laboratory experimental findings, and serve as benchmarks in the present study.

Mean flow characteristics of all the field measurements are given in Table II. For all the analyses, we have invoked Taylor’s hypothesis to convert time series to spatial series.

V. RESULTS

A. Analysis of hot-wire measurements

In this section, hot-wire measurements and their surrogates are analyzed to (a) demonstrate the ability of the magnitude cumulant analysis to accurately estimate the intermittency structure of turbulent velocity series and (b) establish that the surrogate series, while preserving the pdf and spectrum of the original data, destroy the intermittency structure.

In Fig. 3, the magnitude cumulants and second-order structure function computed from the hot-wire measurements of Kunkel and Marusic¹⁶ are shown. This turbulence series is 30 min long ($\sim 18 \times 10^6$ data points) and captures scales down to the Kolmogorov scale. The local slopes of the magnitude cumulants and second-order structure functions (estimated using second-order central differencing) are shown in Fig. 4. The vertical dotted lines in Figs. 3 and 4 represent the scaling range over which c_n ($n=1-3$), and ζ_2 can be reliably estimated using linear regression.

The following observations can be made from Figs. 3–5:

- c_1^{turb} computed from the turbulence velocity signal is close to -0.38 . The 95% confidence interval is $(-0.384, -0.382)$. c_1^{turb} agrees quite well with the existing results from low Re laboratory experiments.^{18,21}
- c_2^{turb} is approximately equal to 0.03. In this case, the 95% confidence interval is $(0.029, 0.032)$. Delour *et al.*¹⁸ and Chevillard *et al.*²¹ reported $c_2 = 0.025 \pm 0.003$ based on several experiments and claimed it to be “universal.” From Eq. (7), we can compute the intermittency exponent $\mu \approx 9 \times c_2^{\text{turb}} \approx 0.27$. In the literature, researchers have reported μ ranging from 0.18 to 0.7.^{10,11} In the case of atmospheric data, the “best” direct estimate is 0.25 ± 0.05 (Ref. 10) and our indirect magnitude cumulant analysis-based result is in agreement with it.
- Figure 5 portrays that c_2^{turb} is converged for sample sizes of approximately 14×10^6 and higher.
- In the inertial range, c_3^{turb} cannot be distinguished from zero [95% confidence interval is $(-0.008, 0.002)$]. This indicates that the statistics of the velocity increments are possibly log-normal.^{18,21} Please see the Appendix for a brief discussion on c_4^{turb} computation.
- Since $c_3^{\text{turb}} \approx 0$ and $c_4^{\text{turb}} \approx 0$, from Eq. (6) we can derive: $\zeta_2^{\text{turb}} = -2c_1^{\text{turb}} - 2c_2^{\text{turb}} = 2 \times 0.38 - 2 \times 0.03 = 0.70$. Figure 3 (bottom-right) shows the second-order structure function. The slope of this plot gives $\zeta_2^{\text{turb}} = 0.70$ [95% confidence interval is $(0.702, 0.706)$]. Thus, our results are self-consistent.
- c_2^{sur} estimated from the surrogate of the measured turbulence velocity series is zero; i.e., the surrogate series is nonintermittent.

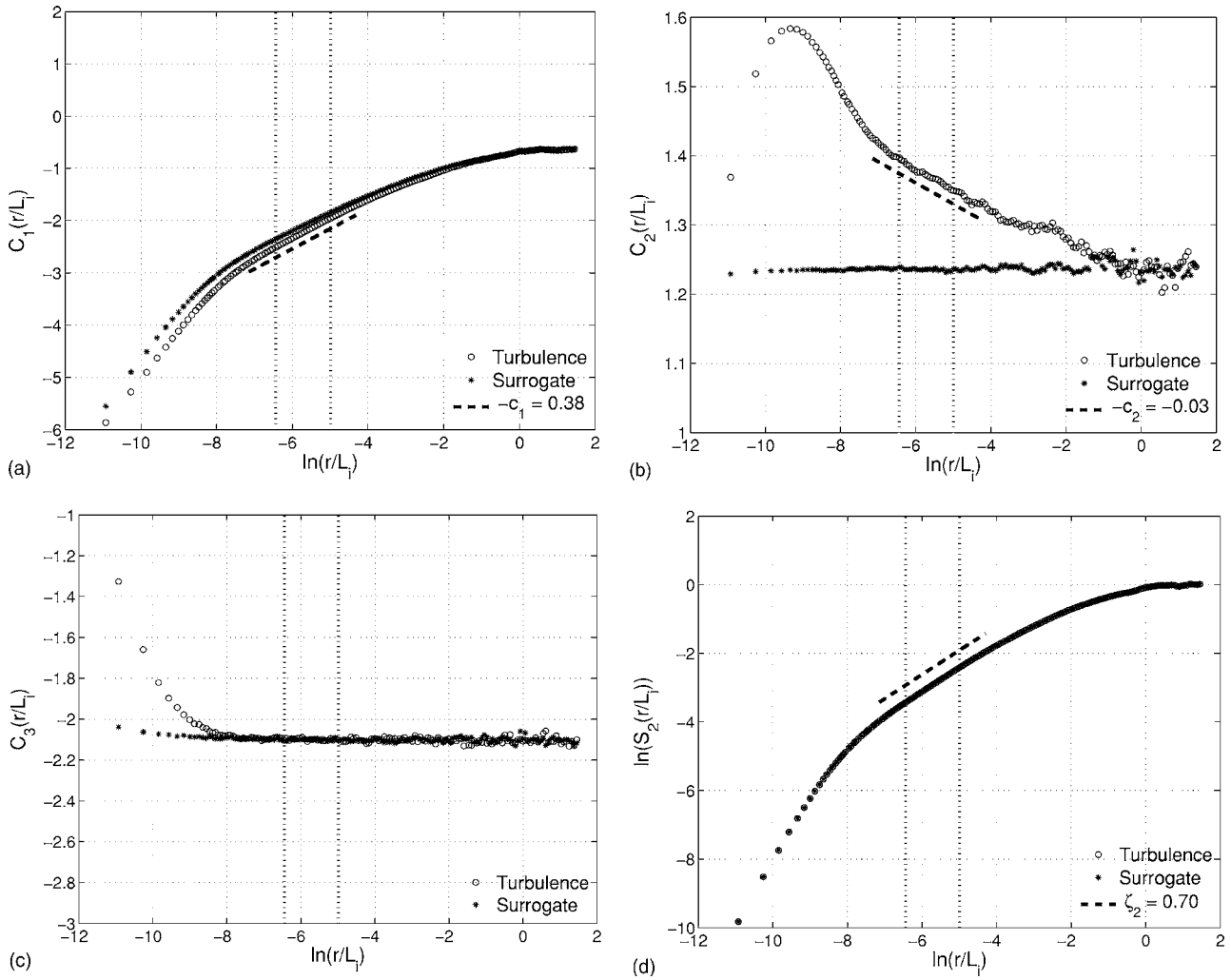


FIG. 3. $C_1(r/L_1)$ (top-left), $C_2(r/L_1)$ (top-right), and $C_3(r/L_1)$ (bottom-left) computed using the hot wire measurements of Kunkel and Marusic (Ref. 16.) The second-order structure function is also shown (bottom-right). The circles denote the statistics corresponding to the original turbulence series and the stars represent the statistics computed from the IAAFT surrogate series. Clearly, the original series portray the signatures of a multifractal process. In contrast, the surrogate series shows the signs of monofractality. The vertical dotted lines represent the scaling range over which c_n ($n=1-3$), and ζ_2 can be reliably estimated. The dashed lines show the slopes $-c_1^{\text{turb}}=0.38$ (top-left), $-c_2^{\text{turb}}=-0.03$ (top-right), and $\zeta_2^{\text{turb}}=0.70$ (bottom-right).

- By construction, the surrogate series (i.e., turbulence without intermittency) preserves the second-order statistics. Thus, $\zeta_2^{\text{turb}} = \zeta_2^{\text{surr}}$. Using this relationship, the fact that $c_2^{\text{surr}} = 0$, and Eq. (6), it is straightforward (since our present data analysis supports that $c_3^{\text{turb}} \approx 0$ and $c_4^{\text{turb}} \approx 0$) to show that: $c_1^{\text{turb}} + c_2^{\text{turb}} = c_1^{\text{surr}}$. In the present case, this results in: $c_1^{\text{surr}} = -0.38 + 0.03 = -0.35$ (see also Fig. 3). Thus, $\zeta_1^{\text{surr}} = -c_1^{\text{surr}} = 0.35$ is in close accord with K41 hypothesis of $\zeta_1 = 1/3$.¹ The relationship $c_1^{\text{turb}} + c_2^{\text{turb}} = c_1^{\text{surr}}$ has significant practical implications. It insinuates that one can roughly estimate c_2^{turb} (and thus μ) by means of first-order magnitude cumulants of turbulence and its corresponding surrogate; i.e., $c_2^{\text{turb}} = c_1^{\text{surr}} - c_1^{\text{turb}}$. In our opinion, for estimating intermittency in short-length geophysical signals, this simple indirect method, which does not require even second-order magnitude cumulant computation, would be quite useful.
- In the turbulence literature, there is a general consensus that $\zeta_3 = 1$. From our results, we find $\zeta_3^{\text{turb}} = -3c_1^{\text{turb}}$

$-9/2c_2^{\text{turb}} = 1.14 - 0.135 = 1.005$, in close agreement with the well-accepted value.

We proceed further by comparing the pdf of the velocity and surrogate increments using the skewness, asymmetry factor, and flatness defined as

$$\text{Skewness}(r) = \frac{\langle(\Delta u)^3\rangle}{\langle(\Delta u)^2\rangle^{3/2}}, \tag{10a}$$

$$\text{Asymmetry}(r) = \frac{\langle(\Delta u)^3\rangle}{\langle|(\Delta u)^3|\rangle}, \tag{10b}$$

$$\text{Flatness}(r) = \frac{\langle(\Delta u)^4\rangle}{\langle(\Delta u)^2\rangle^2}. \tag{10c}$$

From Fig. 6 (left), it is evident that the original turbulence increment series show negative skewness (up to ~ 0.6) for small scales, in accord with the existing literature (e.g.,

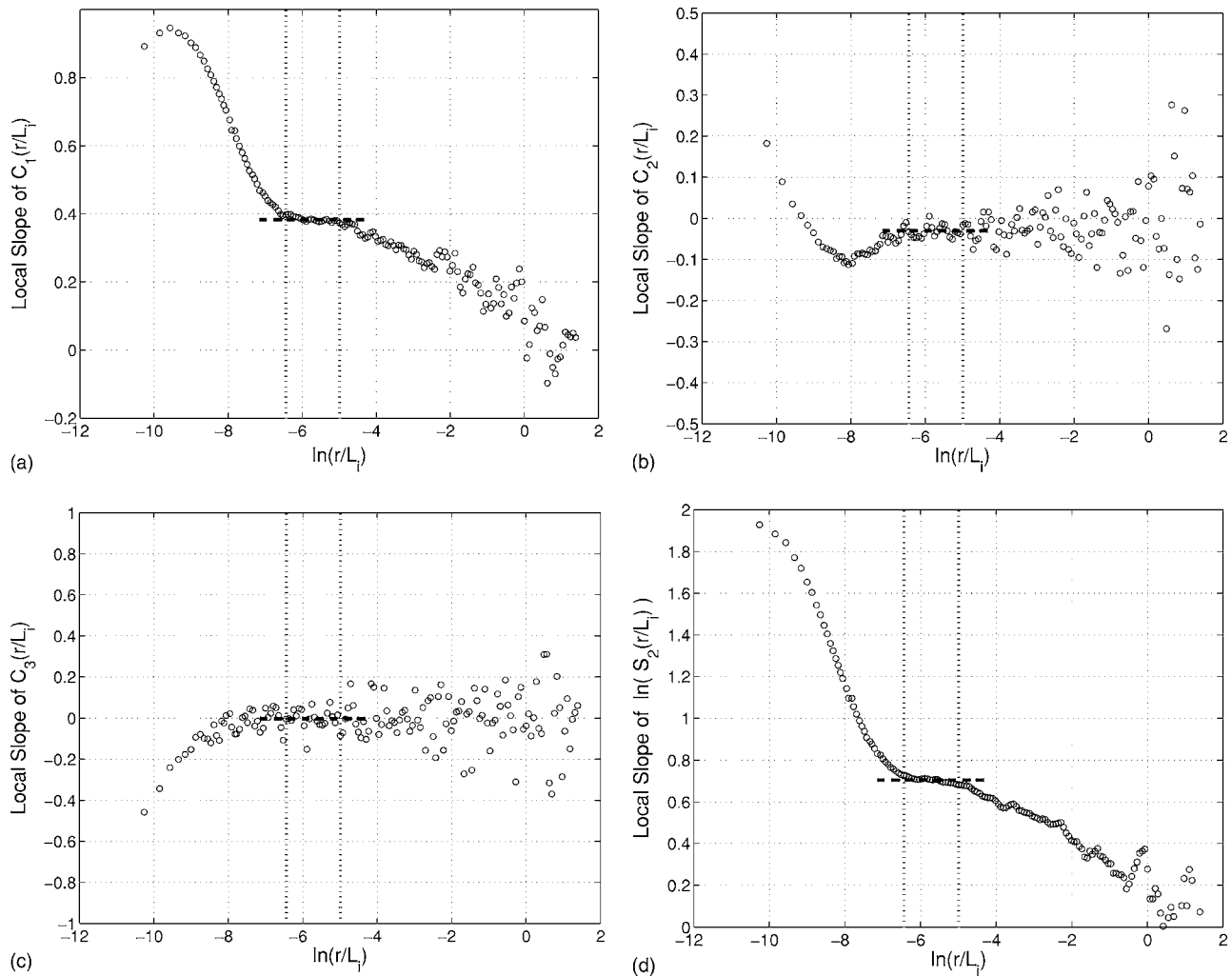


FIG. 4. The local slopes of $C_1(r/L_i)$ (top-left), $C_2(r/L_i)$ (top-right), $C_3(r/L_i)$ (bottom-left), and $\ln[S_2(r/L_i)]$ (bottom-right), for the same turbulence data series used in Fig. 3. Second-order central differencing is used to compute the local slopes. The vertical dotted lines represent the scaling range over which c_n ($n=1-3$), and ζ_2 can be reliably estimated. Computed (linearly regressed) values of $-c_1^{\text{turb}}$ (top-left), $-c_2^{\text{turb}}$ (top-right), $-c_3^{\text{turb}}$ (bottom-left), and ζ_2^{turb} (bottom-right) are shown as horizontal dashed lines.

Chevillard *et al.*²¹). This negative skewness is believed to be related to the vortex folding and stretching process. Malécot *et al.*²² argued that the asymmetry factor [see Eq. (10) for a definition] is a better measure of the asymmetry of the pdf than the skewness. We found that both of these signed odd-order moments behave quite similarly (Fig. 6, left). The origin of spurious oscillations of these odd-order moments for large scales [$\ln(r/L_i) > -4$] is not well understood. The flatness plot (Fig. 6, right) also portrays anticipated characteristics. Flatness corresponding to the integral scale is close to 3 (hallmark of Gaussian velocity increments) and becomes exceedingly large for smaller scales. In contrast, the surrogate shows Gaussian characteristics for all scales. This corroborates the fact that surrogates cannot capture the pdfs of turbulence velocity increments.

B. Analysis of sonic anemometer measurements

Magnitude cumulants and second-order structure functions computed from a sonic anemometer series are shown in Fig. 7. The trends are very similar to Fig. 3, albeit quite noisy. From this figure, we calculated $c_1 = -0.37$, $c_2 = 0.06$,

and $\zeta_2 = 0.63$. We would like to emphasize that even in this short time series scenario, we can reliably detect intermittency with the help of IAAFT surrogate (see Fig. 7, top-right). Admittedly, the estimation of c_2 is possibly not very accurate. The estimation can be improved by using quenched or annealed averaging strategy (discussed below).

It is quite difficult to manually yet objectively select scaling ranges from a large dataset (specifically, 139 near-neutral turbulence series). Thus, we used an automated scaling range of $[4U/f_s L_i/2]$ for individual series. Here, U , f_s , and L_i denote mean velocity, sampling frequency, and integral length scale, respectively. From each individual turbulence series and their surrogates, we calculated the corresponding c_1 and c_2 values. Subsequently, from these 139 c_1^{turb} , c_2^{turb} , c_1^{surr} , and c_2^{surr} combinations, we computed the best estimates (ensemble mean ± 1 standard deviation) as: $\langle c_1^{\text{turb}} \rangle = -0.33 \pm 0.03$, $\langle c_2^{\text{turb}} \rangle = 0.038 \pm 0.017$, $\langle c_1^{\text{surr}} \rangle = -0.30 \pm 0.03$, and $\langle c_2^{\text{surr}} \rangle = 0.002 \pm 0.013$. This averaging strategy is similar to the quenched averaging method used by Arnéodo *et al.*³⁸ The key result: $\langle c_2^{\text{turb}} \rangle \gg \langle c_2^{\text{surr}} \rangle$, without any doubt, once again

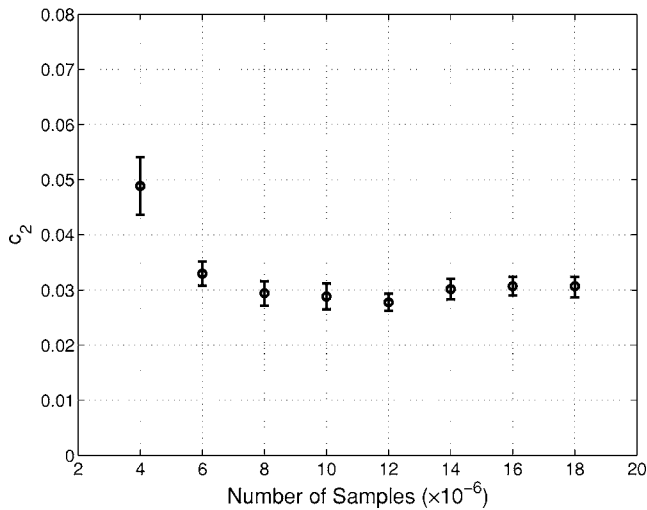


FIG. 5. c_2^{turb} versus sample size for the hot-wire measurements of Kunkel and Marusic (Ref. 16). The error bars denote 95% confidence intervals.

guarantees that the IAAFT surrogates can be faithfully used for turbulence intermittency detection testing.

As an alternative strategy, using the annealed averaging method,³⁸ we have also computed the average of the magnitude cumulants (i.e., $\langle C_1(r/L_i) \rangle$, $\langle C_2(r/L_i) \rangle$) from the same turbulence and surrogate datasets (Fig. 8). From this figure, we estimate the slopes as: $\bar{c}_1^{\text{turb}} = -0.35$, $\bar{c}_2^{\text{turb}} = 0.042$, $\bar{c}_1^{\text{sur}} = -0.31$, $\bar{c}_2^{\text{sur}} = 0.002$. Obviously, there is no significant discrepancy between the quenched and annealed averaged statistics, as would be wishfully expected. Lastly, these statistics highlight that the relationship established in Sec. V A; i.e., $c_1^{\text{turb}} + c_2^{\text{turb}} = c_1^{\text{sur}}$, is also valid under annealed averaging.

VI. CONCLUDING REMARKS AND FUTURE PERSPECTIVES

In this work, we have established a framework based on magnitude cumulant and surrogate analyses to reliably detect the presence of intermittency and estimate the intermittency

coefficient from short turbulent time series. By virtue of this framework, ensemble scaling results extracted from a large number of neutrally stratified atmospheric surface layer turbulent series (predominantly acquired by slow-response sonic anemometers) from various field campaigns remarkably concur with well-known published (mostly laboratory experimental) results.

Neutrally stratified atmospheric surface layer (ASL) turbulence suffers from strong anisotropies due to shear effects. In the recent years, a few turbulence research groups have been trying to disentangle the effects of anisotropy from scaling exponents (e.g., Kurien *et al.*,³⁹ Kurien and Sreenivasan,⁴⁰ Biferale *et al.*,⁴¹ and Staicu *et al.*⁴²). In the context of ASL turbulence, Kurien and Sreenivasan⁴⁰ found that “the anisotropy effects diminish with decreasing scale although much more slowly than previously thought.” Admittedly, the magnitude cumulant analysis does not take into consideration the effects of anisotropy. In the future, we hope to generalize the magnitude cumulant analysis to explicitly account for the anisotropic effects.

The focus of the present study was on neutrally stratified atmospheric turbulence. However, it is widely known that neutral stability conditions are rarely encountered in the real atmosphere. Most of the time, the atmospheric boundary layer is strongly modulated by buoyancy. It is commonly assumed that the effect of atmospheric stability is felt only at the “buoyancy range,” which has scales considerably larger than the inertial range. Recently, Aivalis *et al.*⁴³ studied the intermittency behavior of temperature in the convective surface layer using cold wire anemometry. They found that the classical inertial range remains intact in convective surface layer and the scaling exponents approach values appropriate to the intermittent case of isotropic turbulence. They also noticed that the scaling exponents corresponding to the buoyancy range are highly anomalous. In contrast, Shi *et al.*⁴⁴ found that in the case of temperature, the inertial range scaling exponents are unambiguously impacted by atmospheric stability. However, their results are inconclusive

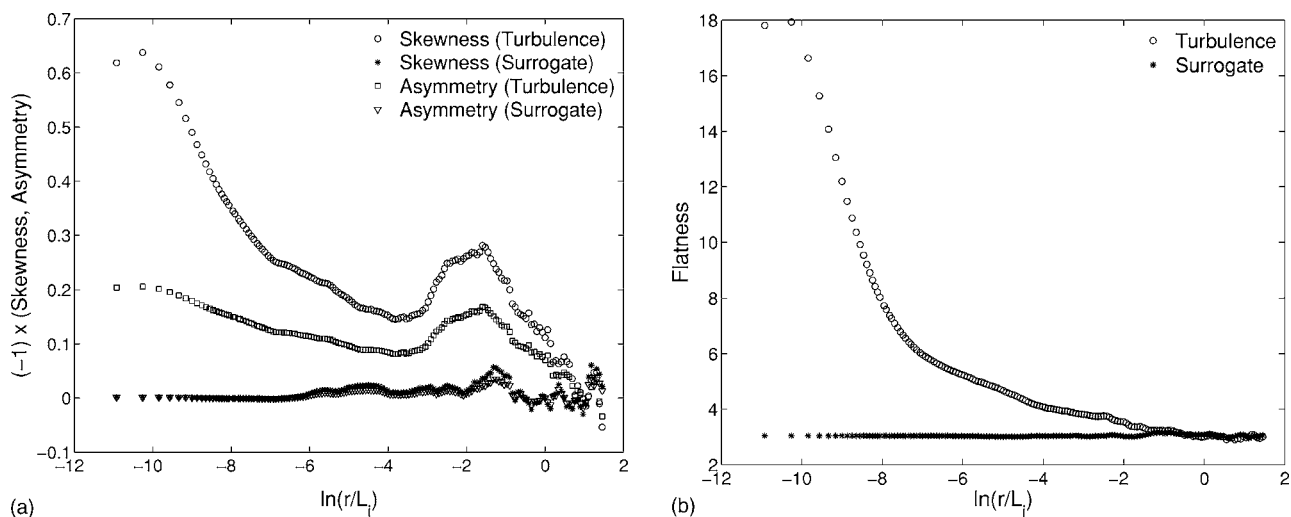


FIG. 6. Negative skewness, asymmetry factor (left), and flatness (right) of the longitudinal velocity increments and the increments of the surrogate series. We utilized the hot-wire measurements of Kunkel and Marusic (Ref. 16).

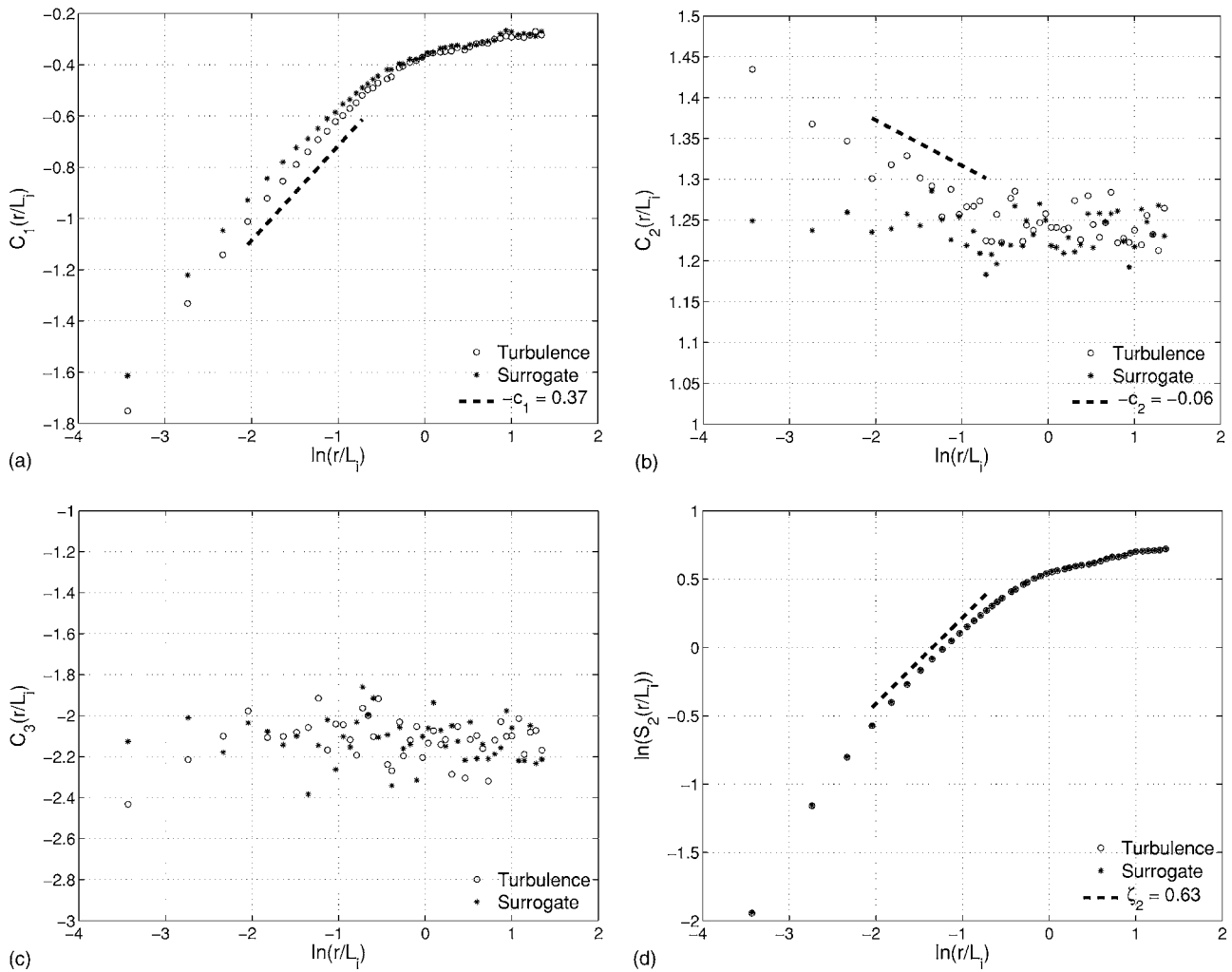


FIG. 7. Same as Fig. 3, but estimated from a sonic anemometer series.

in the case of velocity signals under different stability regimes. We believe that the unresolved question as to whether or not the inertial-range intermittency is influenced by large-scale anisotropic forcing of atmospheric stability is of great

consequence and needs further consideration. Abundant high-quality slow response data collected under different atmospheric regimes in recent years (e.g., Cooperative Atmosphere-Surface Exchange Study - CASES99⁴⁵) could

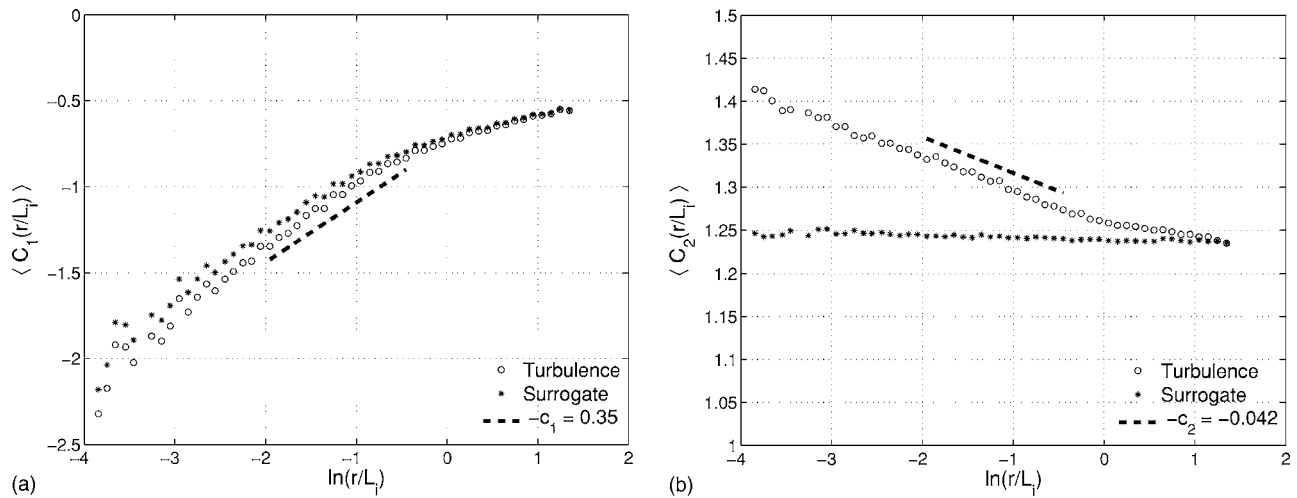


FIG. 8. Ensemble averaged $C_1(r/L_i)$ and $C_2(r/L_i)$ plots from 139 near-neutral turbulence series (circles) and corresponding surrogates (stars). The dashed lines show the slopes $-c_1^{\text{turb}} = 0.35$ (left) and $-c_2^{\text{turb}} = -0.042$ (right).

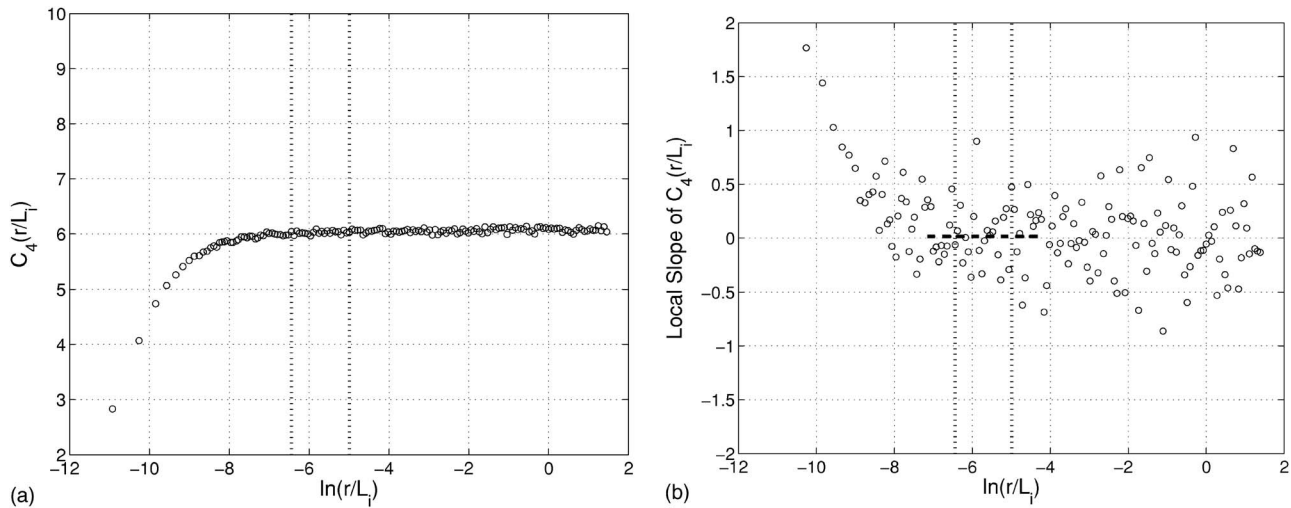


FIG. 9. $C_4(r/L_i)$ (left) computed using the hot-wire measurements of Kunkel and Marusic (Ref. 16). The local slopes of $C_4(r/L_i)$ for the same data series is shown in the right subplot. The vertical dotted lines represent the scaling range over which c_n ($n=1-3$), and ζ_2 have been reliably estimated (see Figs. 3 and 4).

be coupled with the robust scaling analysis and estimation framework explored in this study in order to shed new light into this fundamental problem.

ACKNOWLEDGMENTS

We would like to thank Gary Kunkel and Ivan Marusic for providing us with the hot-wire measurements taken at the SLTEST facility, Utah. We are also grateful to all the researchers who painstakingly collected data during the Davis field campaigns. This work was partially funded by the National Science Foundation (ANT-0538453) and the Texas Advanced Research Program (003644-0003-2006) grants awarded to S.B. E.F.-G. acknowledges support by NASA, under its Global Precipitation Mission (GPM) program, and by NSF via the National Center for Earth-surface Dynamics (NCED) under agreement EAR-0120914.

APPENDIX: c_4^{turb} COMPUTATION

For a log-normal process, $c_n=0$ for $n \geq 3$. In Sec. V, we found that $c_3^{\text{turb}} \approx 0$, which could be speculated as a signature of an underlying log-normal process. However, in order to be more certain, one needs to compute higher order cumulants. In this Appendix, we attempt to compute c_4^{turb} from the hot-wire measurements of Kunkel and Marusic.¹⁶ $C_4(r)$ can be written as

$$C_4(r) \equiv \langle (\ln|\Delta u|)^4 \rangle - 4\langle (\ln|\Delta u|)^3 \rangle \langle \ln|\Delta u| \rangle - 3\langle (\ln|\Delta u|)^2 \rangle^2 + 12\langle (\ln|\Delta u|)^2 \rangle \langle (\ln|\Delta u|) \rangle^2 - 6\langle (\ln|\Delta u|) \rangle^4 \sim -c_4 \ln(r) \quad (\text{A1})$$

From Fig. 9 (left), it seems that $C_4(r/L_i)$ is approximately flat in the inertial range (i.e., $c_4^{\text{turb}} \approx 0$). However, the local slopes of $C_4(r/L_i)$ are overly scattered to provide any conclusive evidence of log-normality (see Fig. 9, right). Estimation of higher order magnitude cumulants require astronomical amount of statistical samples. We would like to note that Arnéodo *et al.*⁴⁶ utilized a turbulence series of length

25×10^7 points (approximately 14 times larger than the hot-wire sample size used in the present study) and still was unable to reach statistical convergence for c_4 and higher-order cumulants.

- ¹U. Frisch, *Turbulence* (Cambridge University Press, Cambridge, UK, 1995), p. 296.
- ²D. Schertzer, S. Lovejoy, F. Schmitt, Y. Chigirinskaya, and D. Marsan, "Multifractal cascade dynamics and turbulent intermittency," *Fractals* **5**, 427 (1997).
- ³A. Scotti and C. Meneveau, "A fractal model for large eddy simulation of turbulent flow," *Physica D* **127**, 198 (1999).
- ⁴H. F. Campos Velho, R. R. Rosa, F. M. Ramos, R. A. Pielke, G. A. Degrazia, C. Rodrigues Neto, and A. Zanandrea, "Multifractal model for eddy diffusivity and counter-gradient term in atmospheric turbulence," *Physica A* **295**, 219 (2001).
- ⁵S. Basu, E. Foufoula-Georgiou, and F. Porté-Agel, "Synthetic turbulence, fractal interpolation, and large-eddy simulation," *Phys. Rev. E* **70**, 026310 (2004).
- ⁶M. Antonelli, M. Martins Afonso, A. Mazzino, and U. Rizza, "Structure of temperature fluctuations in turbulent convective boundary layers," *J. Turbul.* **6**, 3510.1080/14685240500332049 (2005).
- ⁷G. C. Burton and W. J. A. Dahm, "Multifractal subgrid-scale modeling for large-eddy simulation. I. Model development and a priori testing," *Phys. Fluids* **17**, 075111 (2005).
- ⁸A. Monin and A. Yaglom, *Statistical Fluid Mechanics* (MIT Press, Cambridge, MA, 1975), Vol. 2, p. 874.
- ⁹C. Meneveau and K. R. Sreenivasan, "The multifractal nature of the turbulent energy dissipation," *J. Fluid Mech.* **224**, 429 (1991).
- ¹⁰K. R. Sreenivasan and P. Kailasna, "An update on the intermittency exponent in turbulence," *Phys. Fluids A* **5**, 512 (1993).
- ¹¹A. Praskovsky and S. Oncley, "Comprehensive measurements of the intermittency exponent in high Reynolds number turbulent flows," *Fluid Dyn. Res.* **21**, 331 (1997).
- ¹²J. Cleve, M. Greiner, B. R. Pearson, and K. R. Sreenivasan, "Intermittency exponent of the turbulent energy cascade," *Phys. Rev. E* **69**, 066316 (2004).
- ¹³F. Anselmetti, Y. Gagne, E. J. Hopfinger, and R. A. Antonia, "High-order velocity structure functions in turbulent shear flows," *J. Fluid Mech.* **140**, 63 (1984).
- ¹⁴A. J. Chambers and R. A. Antonia, "Atmospheric estimates of power-law exponents," *Boundary-Layer Meteorol.* **28**, 343 (1984).
- ¹⁵I. Marusic and G. J. Kunkel, "Streamwise turbulence intensity formulation for flat-plate boundary layers," *Phys. Fluids* **15**, 2461 (2003).

- ¹⁶G. J. Kunkel and I. Marusic, "Study of the near-wall-turbulent region of the high-Reynolds-number boundary layer using an atmospheric flow," *J. Fluid Mech.* **548**, 375 (2006).
- ¹⁷U. Frisch, P.-L. Sulem, and M. J. Nelkin, "A simple dynamical model of intermittent fully developed turbulence," *J. Fluid Mech.* **87**, 719 (1978).
- ¹⁸J. Delour, J. F. Muzy, and A. Arnéodo, "Intermittency of 1D velocity spatial profiles in turbulence: A magnitude cumulant analysis," *Eur. Phys. J. B* **23**, 243 (2001).
- ¹⁹T. Schreiber and A. Schmitz, "Improved surrogate data for nonlinearity tests," *Phys. Rev. Lett.* **77**, 635 (1996).
- ²⁰T. Bohr, M. H. Jensen, G. Paladin, and A. Vulpiani, *Dynamical Systems Approach to Turbulence* (Cambridge University Press, Cambridge, UK, 1998), p. 350.
- ²¹L. Chevillard, B. Castaing, E. Lévêque, and A. Arnéodo, "Unified multifractal description of velocity increments statistics in turbulence: Intermittency and skewness," *Physica D* **218**, 77 (2006).
- ²²Y. Malécot, C. Auriault, H. Kahalerras, Y. Gagne, O. Chanal, B. Chabaud, and B. Castaing, "A statistical estimator of turbulence intermittency in physical and numerical experiments," *Eur. Phys. J. B* **16**, 549 (2000).
- ²³V. Venugopal, S. G. Roux, E. Foufoula-Georgiou, and A. Arnéodo, "Scaling behavior of high resolution temporal rainfall: New insights from a wavelet-based cumulant analysis," *Phys. Lett. A* **348**, 335 (2006).
- ²⁴V. Venugopal, S. G. Roux, E. Foufoula-Georgiou, and A. Arnéodo, "Revisiting multifractality of high-resolution temporal rainfall using a wavelet-based formalism," *Water Resour. Res.* **42**, W06D1410.1029/2005WR004489 (2006).
- ²⁵J. F. Muzy, E. Bacry, and A. Arnéodo, "Multifractal formalism for fractal signals: The structure-function approach versus the wavelet-transform modulus-maxima method," *Phys. Rev. E* **47**, 875 (1993).
- ²⁶A. Arnéodo, E. Bacry, and J. F. Muzy, "The thermodynamics of fractals revisited with wavelets," *Physica A* **213**, 232 (1995).
- ²⁷J. F. Muzy, E. Bacry, and A. Arnéodo, "Wavelets and multifractal formalism for singular signals: Application to turbulence data," *Phys. Rev. Lett.* **67**, 3515 (1991).
- ²⁸M. Vergassola, R. Benzi, L. Biferale, and D. Pisarenko, "Wavelet analysis of a Gaussian Kolmogorov signal," *J. Phys. A* **26**, 6093 (1993).
- ²⁹J. Theiler, S. Eubank, A. Longtin, B. Galdrikian, and J. D. Farmer, "Testing for nonlinearity in time series: the method of surrogate data," *Physica D* **58**, 77 (1992).
- ³⁰H. Kantz and T. Schreiber, *Nonlinear Time Series Analysis* (Cambridge University Press, Cambridge, UK, 1997), p. 320.
- ³¹S. Basu and E. Foufoula-Georgiou, "Detection of nonlinearity and chaos in time series using the transportation distance function," *Phys. Lett. A* **301**, 413 (2002).
- ³²V. Venema, F. Ament, and C. Simmer, "A stochastic iterative amplitude adjusted Fourier transform algorithm with improved accuracy," *Nonlinear Processes Geophys.* **13**, 247 (2006).
- ³³V. Venugopal, S. Basu, and E. Foufoula-Georgiou, "A new metric for comparing precipitation patterns with an application to ensemble forecasts," *J. Geophys. Res.* **110**, D0811110.1029/2004JD005395 (2005).
- ³⁴V. Venema, S. Meyer, S. G. García, A. Kniffka, C. Simmer, S. Crewell, U. Löhnert, T. Trautmann, and A. Macke, "Surrogate cloud fields generated with the iterative amplitude adapted Fourier transform algorithm," *Tellus, Ser. A* **58A**, 104 (2006).
- ³⁵V. Nikora, D. Goring, and R. Camussi, "Intermittency and interrelationships between turbulence scaling exponents: Phase-randomization tests," *Phys. Fluids* **13**, 1404 (2001).
- ³⁶M. Pahlow, M. B. Parlange, and F. Porté-Agel, "On Monin Obukhov similarity in the stable atmospheric boundary layer," *Boundary-Layer Meteorol.* **99**, 225 (2001).
- ³⁷S. Basu, F. Porté-Agel, E. Foufoula-Georgiou, J.-F. Vinuesa, and M. Pahlow, "Revisiting the local scaling hypothesis in stably stratified atmospheric boundary-layer turbulence: An integration of field and laboratory measurements with large-eddy simulations," *Boundary-Layer Meteorol.* **119**, 473 (2006).
- ³⁸A. Arnéodo, N. Decoster, and S. G. Roux, "A wavelet-based method for multifractal image analysis. I. Methodology and test applications on isotropic and anisotropic random rough surfaces," *Eur. Phys. J. B* **15**, 567 (2000).
- ³⁹S. Kurien, V. S. L'vov, I. Procaccia, and K. R. Sreenivasan, "Scaling structure of the velocity statistics in atmospheric boundary layer," *Phys. Rev. E* **61**, 407 (2000).
- ⁴⁰S. Kurien, and K. R. Sreenivasan, "Anisotropic scaling contributions to high-order structure functions in high-Reynolds-number turbulence," *Phys. Rev. E* **62**, 2206 (2000).
- ⁴¹L. Biferale, D. Lohse, I. M. Mazzitelli, and F. Toschi, "Probing structures in channel flow through SO(3) and SO(2) decomposition," *J. Fluid Mech.* **452**, 39 (2002).
- ⁴²A. Staicu, B. Vorselaars, and W. van de Water, "Turbulence anisotropy and the SO(3) description," *Phys. Rev. E* **68**, 046303 (2003).
- ⁴³K. G. Aivalis, K. R. Sreenivasan, J. C. Klewicki, and C. A. Biloft, "Temperature structure functions for air flow over moderately heated ground," *Phys. Fluids* **14**, 2439 (2002).
- ⁴⁴B. Shi, B. Vidakovic, G. G. Katul, and J. D. Albertson, "Assessing the effects of atmospheric stability on the fine structure of surface layer turbulence using local and global multiscale approaches," *Phys. Fluids* **17**, 055104 (2005).
- ⁴⁵G. S. Poulos, W. Blumen, D. C. Fritts, J. K. Lundquist, J. Sun, S. P. Burns, C. Nappo, R. Banta, R. Newsom, J. Cuxart, E. Terradellas, B. Balsley, and M. Jensen, "CASES-99: A comprehensive investigation of the stable nocturnal boundary layer," *Bull. Am. Meteorol. Soc.* **83**, 555 (2002).
- ⁴⁶A. Arnéodo, S. Manneville, J. F. Muzy, and S. G. Roux, "Revealing a lognormal cascading process in turbulent velocity statistics with wavelet analysis," *Philos. Trans. R. Soc. London, Ser. A* **357**, 2415 (1999).